LVRT Capability Assessment of Grid Code Frequency Responsive VSWTG

Asma Aziz and Aman MTO
Deakin University, Australia
Email: aazi@deakin.edu.au

Alex Stojcevski
RMIT, Vietnam

***Abstract*—With increasing wind energy penetration and impending grid codes, it is important to enable wind based power plants to provide sensitive frequency active power response as well as connection capability during and after a short-term fault. Conventionally active power is given low priority during voltage disturbance and voltage ride through capability is assessed separately with frequency ride through capability. This paper assess the LVRT capability of frequency grid code compatible DFIG based VSWTG under frequency dependent power set-point neglecting current priority. Simulation tests conducted for a weak system shows improved LVRT capability of frequency responsive VSWTGs in comparison to normal VSWTGs. With active power output well above zero and turbine speed also remaining under limit during fault conditions, frequency grid code compatible VSWTGs can also satisfy FRT grid codes of many countries.**

***Index Terms*—DFIG, frequency responsive, grid code, LVRT capability, voltage disturbance**

I. Introduction

Prospective energy security with cost effective levelised cost has given wind an extra attractive proposition in current global scenario as a major contributor for the foreseeable future. Robust participation in electrical grid calls for stable and reliable contribution from wind based power plants. Frequency regulation and voltage stability are two key ancillary services desired from every generating power plants. With increasing wind energy penetrations in modern power system, all national TSOs have put stringent ride through capability limits on these power systems. Fault Ride Through (FRT) capability refers to the generators proficiency in remaining grid connected during balanced and unbalanced short term electrical faults and continuing stable operation in the transmission grid. This constraint has been enforced as mandatory to evade substantial wind energy generation loss in the occasion of grid faults. Earlier trend of disconnection of wind farms pose significant damage to frequency and voltage regulation leading to black out in case of major fault. Besides having maximum power extraction capability with variable speed operation, type 3 and type 4 Variable Speed Wind Turbine Generators (VSWTG) have four-quadrant active and reactive power capability. However, these VSWTGs exhibit very sensitive response to electrical network disturbances, predominantly to voltage sags. Voltage loss leads to magnetization loss and consequent high current flow through stator and rotor circuits of induction generator based VSWTG. These high inrush currents can damage power electronics based converters necessitating disconnection or current bypassing to ride through disturbance and avoid damages. Voltage disturbance due to grid faults leads to transient over-currents in rotor circuit and temporary power control loss in DFIG based VSWTG. Protecting methods are imperative during transient fault periods to save the system from damage due to overcurrent or dc over voltage. Type of protective methods, application duration and efficiency are widely researched topics for DFIG FRT response. [1]-[7]. Voltage drop at generator terminals is normally minimized by applying STATCOMs at wind farm level while rotor over currents mitigation methods are applied at wind turbine level such that currents through the power electronics based converters are always below the surge capability. Restoration of active and reactive power control with grid compliance is also a vital requirement these days. Swift and efficient active and reactive power control restoration subsequent to fault clearance can contribute highly to stable system frequency and fault response of other connected devices in network. Active crowbar is the most commonly applied mitigation method for converter over current protection. Resistance-thyristor based active crowbar short circuits the rotor enabling overcurrent flow through crowbar resistance thus absorbing initial energy outflow and reducing rotor flux decay time period. Rapid demagnetization of rotor protects the rotor converter from further damage. Even though being widely applied method, resistance crowbar suffers from sluggish connection time and loss of generator control. Vector control is lost during crowbar connection and DFIG operation changes as high slip operating induction machine with poor operating torque and reactive power absorption. Complete demagnetization of rotor requires crowbar application for longer duration. [8], [9]. Grid code FRT requirements are

Manuscript received November 21, 2016; revised May 30, 2017.

doi: 10.18178/ijoee.5.1.14-21

impeded during typical crowbar activation till 120 ms can have 100ms post fault period with respect to absorption of reactive power and corresponding voltage drop [10]. Various methods have been proposed to improve crowbar sluggish operating time response and reduced dc voltage ripples. Hysteresis current control scheme with battery support is one of these methods. In normal operation, active power support is a priority. Low Voltage Ride Through capability (LVRT) threshold can vary from 0.8-0.9 p.u contingent on the wind turbine design. Normal wind turbine operation is suspended whenever the turbine voltage drops below this threshold and reactive current is injected into the grid. Active power control is lower priority during this disturbance period and reference active power is set to zero [11]. Voluminous literature exists for individual synthetic inertial support and centralized controlled low frequency response schemes [12]-[18] from power electronics based wind farms during generation-demand mismatch. However, their proficiency throughout the grid faults is ambiguous owing to the ride-through capability of power electronics based converter topology during severe disturbances. While frequency response competencies are typically evaluated as a consequence of generator outage events in a network, this paper investigates the LVRT capability of frequency sensitive type 3 VSWTG and shows that grid code frequency responsive VSWTG have better fault ride through capability without incorporation of any additional hardware like crow circuit. MATLAB based simulations are conducted to present the results

II. FRT Grid Code Requirement

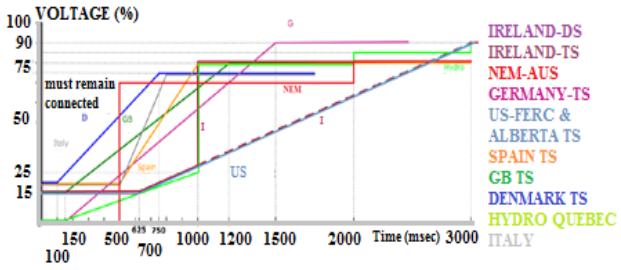

Figure 1. Fault ride through grid codes [19].

FRT requirements defined in various countries grid codes for connection and operation of transmission systems is shown in Fig. 1. Joint consensus of these grid codes demand stable operation from all new generators under a range of defined credible grid faults and time duration. As represented in Fig. 1, voltage drop level varies between 20%-0% of nominal voltage value while minimum fault duration during these voltage drop varies from 100 msec (in Denmark) to 625 msec (in Ireland, USA and Canada. Most stringent requirement for FRT is in Germany which seeks 0% volts for 150 ms (Germany) while Ireland's code is challenging in terms of fault duration of 100ms for 15% volt. Except Australia, technical standards defined in almost all these countries grid code are either at a fixed level or at a level determined by the transmission system operator. The Australian NEM Standard for FRT [20] is classified as the automatic standard which require voltage ride through capability in the range of 80%-90% of nominal voltage for 10 seconds. Most wind generators cannot meet this and therefore comply with a lesser minimum standard of 0% volt for 430msec. Generating unit reactive power support to local voltage is expected during fault period and fault recovery period. Reactive current injection up to 100% during fault is also desired in grid codes of countries like Spain, Germany and Great Britain.

III. Frequency Responsive VSWTG Model

Long term frequency support from VSWTG requires a different auxiliary control algorithm for active power set point provision in individual wind turbine generator instead of MPPT set point. Frequency responsive wind plants provide controllable on-demand power as spinning reserve power in reaction to network frequency deviations scenario. Authors have developed frequency controller model incorporating a grid frequency processor algorithm based on dynamic dead-band around moving averaged frequency instead of conventional static dead-band. The frequency response controller as shown in Fig. 2 generate continuously varying, frequency sensitive active power reference set point for VSWTG according to different grid codes.

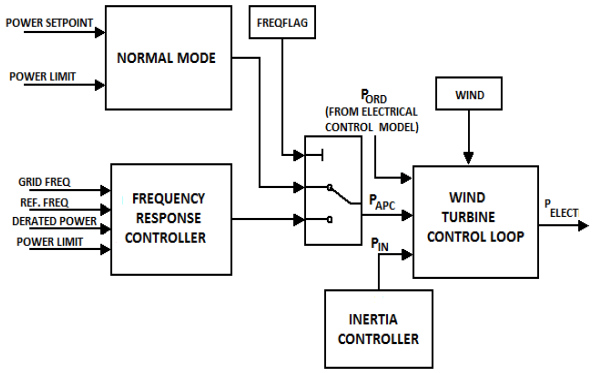

Figure 2. Frequency controlled operation of type 3 VSWTG.

In normal mode no reaction is provided to any frequency deviation and active power set point for wind turbine is managed only according to MPPT and TSO power demand limit. Virtual inertia controller provides inertial power set point to the wind turbine control loop. All the fault ride through technique including crowbar assumes wind turbines operation in MPPT mode. With frequency controllers, VSWTG operates in spinning reserve mode and provides an active power set point P_{APC} to VSWTG torque-pitch controller. In conventional DFIG model, rated power is provided to pitch compensator while we provide P_{APC} as one of the input other than generated electrical power. This frequency controller block provide two types of frequency response according to grid code as shown in Fig. 3. Power set-point will change proportionally to both up and down frequency deviation from reference frequency signal in frequency sensitive response mode while in limited frequency sensitive response mode, active power varies whenever the system frequency exceeds set upper limit otherwise

rated power set-point of according to TSO limitation and demand set-point is provided to WTG turbine controller. Power set points as generated are shown in Fig. 4 corresponding to reference frequency given in Fig. 5. Simplified schematic diagram representing Type 3 (Doubly fed asynchronous generator) based WTG control structure is presented in Fig. 6. Turbine control system involves two control loops having speed error as input and two control outputs: 1. Wind turbine reference power provided to the converter control. 2. Pitch reference value. Rotor speed is controlled at optimum level as per wind power command through torque limitation in speed control loop while mechanical power and corresponding shaft speed of wind turbine is controlled through pitch controller and pitch compensation loop when rotor speed exceeds optimum level.

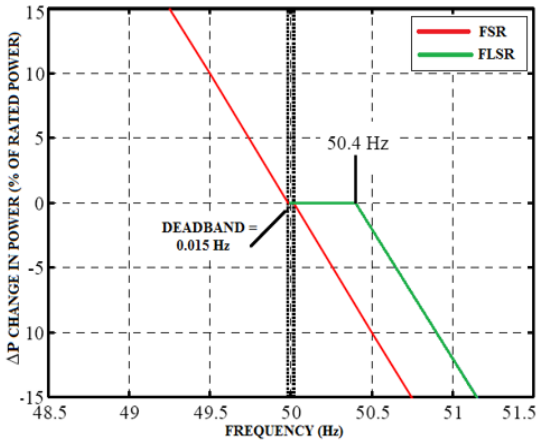

Figure 3. Applied frequency grid code [21].

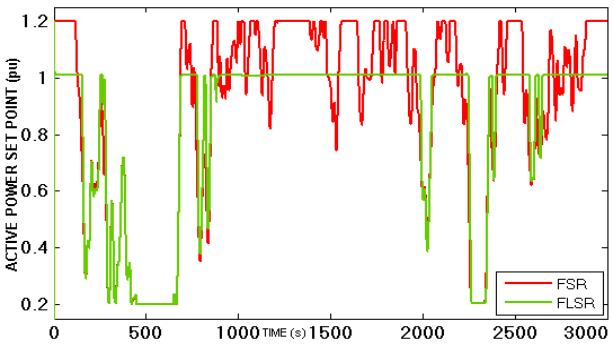

Figure 4. Active power set point generated by frequency response controller-I.

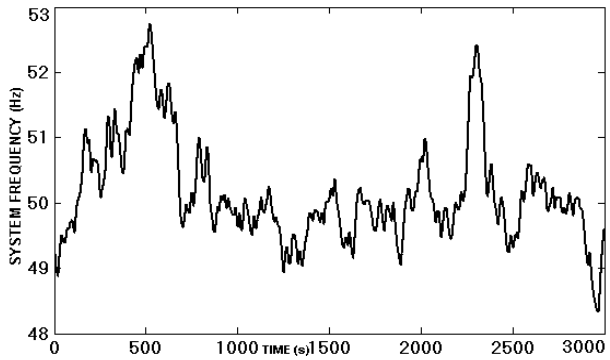

Figure 5. System frequency used to depict frequency response controller-I operation in two different mode.

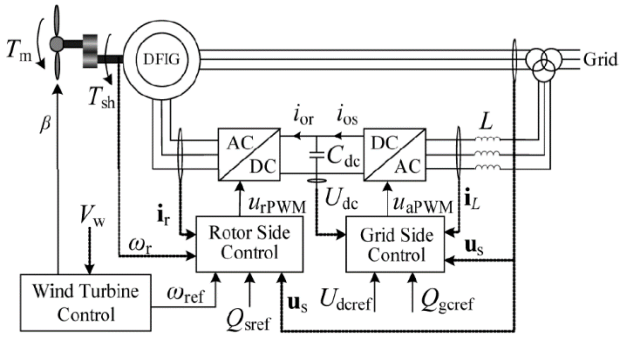

Figure 6. DFIG control structure.

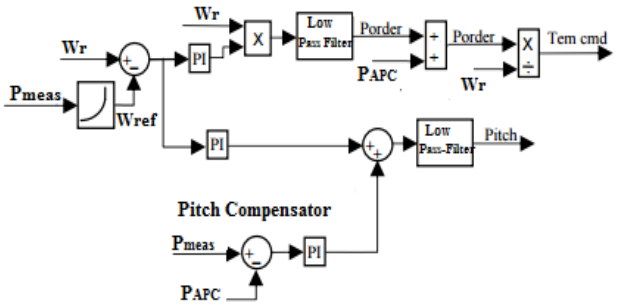

Figure 7. Pitch and torque-speed controller.

Pitch control as shown in Fig. 7, enables optimum control of aerodynamic wind power by rotor blade pitching in order to regulate turbine torque. Maximum power of 1.2 per unit is available at zero pitch angle while it is highly reduced with highest pitch angle. Pitch angle is obtained through PI regulator and it is mathematically expressed by following equations:

$$\theta_{cmd} = \frac{d(K_{ip}(\omega - \omega_{ref}))}{dt} + \frac{d(K_{ic}(P_{\max} - P_{set}))}{dt} + K_{pp}(\omega - \omega_{ref}) + K_{pc}(P_{\max} - P_{APC})$$

where angular reference speed is approximated as:

$$\omega_{ref} = -0.67P_{elect}^2 + 1.42P_{elect} + 0.51$$

under the assumption $0.15\,p.u \le P_{elect} \le 0.75\,p.u$

For $P_{elect} \ge 0.75\,p.u, \omega_{ref} = 1.2\,p.u;$ *and*

$P_{elect} \le 0.15\,p.u, \omega_{ref} = 0.689\,p.u$

More details about the model can be referred from [22]. Pitch compensation block takes active power set-point P_{APC} generated from frequency responsive controller instead of rated reference power.

Frequency dependent power set point will produce demagnetizing current during fault condition which is added to reference rotor current. Final Power order can be altered by passing active power set-point either at turbine torque speed controller loop as shown in Fig. 7 or at rotor side converter control as given in Fig. 8. Final power order can be generated by adding limited active power set point from frequency response controller block to the

power order from speed controller. Power order provided to converter control can also be transformed in accordance with inertia controller to exploit the rotating masses stored energy along with frequency responsive active power command. Optimum speed is maintained corresponding to active power set-point through torque-speed controller. Pitch controller initiates blade pitching in case speed increases and reduces mechanical power thereby reducing speed.

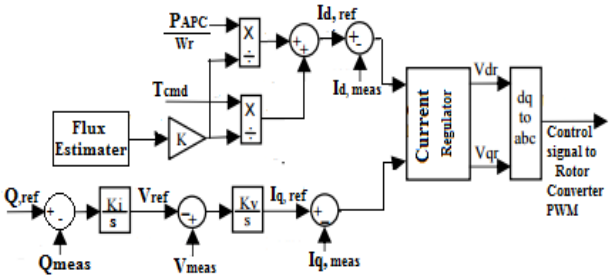

Figure 8. Rotor side converter control.

DFIG control is disseminated intogrid side converter (GSC) and the rotor side converter (RSC) controls. Feed Forward decoupled voltage control is applied in both of these converters for an independent tuning of active and reactive current. DFIG active and reactive power is controlled independently through RSC to adjust the generator speed according to frequency responsive set point operation. Fig. 8 illustrates rotor converter controller comprising of electromagnetic torque and reactive power control. Phase-locked loop is used to align positive sequence of stator voltage with d-axis of the rotating reference frame. The reference electromagnetic torque (T_{cmd}) and frequency responsive torque command ($\frac{P_{APC}}{\omega_r}$) is divided by generator q-axis scaled flux and summated to obtain the reference rotor current i_{dref}. This current is injected in rotor through rotor converter. PI based current regulator is applied to reduce any error between i_{dmeas} and i_{dref} while voltage V_{dr} is obtained as output. In grid converter, VSWTG measured reactive is compared to its reference value (Q_{ref}) and any error is minimized to zero through an integral var regulator. Reference voltage V_{ref} at the VSWTG grid terminals is obtained as output of the var regulator which is compared with actual voltage and any error is regulated an integral regulator. i_{qref} is obtained as output from this current regulator to be injected in rotor by rotor converter. i_q current is regulated to its reference value by applying similar current regulator as for the electromagnetic torque control. Voltage v_{qr} is obtained as the output of the current controller which that will be generated by rotor converter. $dq\ to\ ABC$ transformation is then performed to obtain the 3-phase voltage rotor converter.

IV. DFIG Voltage Oriented Decoupled Control

Owing to direct grid tied coupling of stator winding, Stator Voltage Oriented Control (SVOC) technique is one of the convenient method for DFIG decoupled control operation [23]-[25] for active and reactive power. The three phase signals in abc stationary frame are transformed into two phase active and reactive signals in dq synchronous frame. Decoupled control involves independent control of these two active and reactive components. The synchronous reference frame's d axis is aligned with stator voltage vector v_s in stator voltage oriented control. The resultant d and q axis stator voltage are $v_{ds} = v_s$ and $v_{qs} = \sqrt{{v_s}^2 - {v_{ds}}^2} = 0$ Rotor voltage and current can also be resolved into dq axis components and independently controlled through rotor converter. Electromagnetic torque which is generally used for active power control can be expressed as function of stator flux linkage and rotor current in dq axis as:

$$T_e = \frac{3PL_m}{2L_S}(-i_{qr}\lambda_{ds} + i_{dr}\lambda_{qs}) \quad (1)$$

Stator voltage in dq-axis during steady state operation is given as:

$$v_S = (v_{ds} + jv_{qs}) = R_S(i_{ds} + ji_{qs}) + j\omega_S(\lambda_{ds} + j\lambda_{qs}) \quad (2)$$

After obtaining dq-axis flux value from equation 2 and substituting it into equation 1 will give:

$$T_e = \frac{3PL_m}{2\omega_S L_S}(-i_{qr}v_{qs} + R_S i_{qs} i_{qr} + R_S i_{ds} i_{dr} - v_{ds} i_{dr})$$

Putting $v_{qs} = 0$ for SVOC will result in simplified electromagnetic torque as:

$$T_e = \frac{3PL_m}{2\omega_S L_S}(R_S i_{qs} i_{qr} + R_S i_{ds} i_{dr} - v_{ds} i_{dr}) \quad (3)$$

Neglecting low stator resistance value will provide simplified electromagnetic torque as a function of d-axis rotor current and stator voltage:

$$T_e = \frac{3PL_m}{2\omega_S L_S} v_{ds} i_{dr} \quad (4)$$

Torque producing component of rotor current is d-axis rotor current i_{dr}^* can be calculated from the torque equation 4 as:

$$T_e = \frac{3PL_m}{2\omega_S L_S} i_{dr}^* v_{ds} \quad (5)$$

The q-axis rotor reference current i_{qr}^* for a given stator reactive power reference Q_s^* can be calculated as:

$$i_{qr}^* = \frac{2L_S}{3v_{ds}L_m} Q_s^* - \frac{v_{ds}}{\omega_S L_m} \quad (6)$$

The dq-axis reference currents i_{dr}^{*} and i_{qr}^{*} are further compared with measured values and errors passed through PI controllers. The dq-axis rotor reference voltage thus obtained as PI controller output are then transformed in three phase rotor voltages in stationary frame. These transformed reference voltages then act as modulating signal in PWM based modulation. The grid side converter with its decoupled controller maintain constant DC link voltage and supplies reactive power to the grid. Grid voltage and angle is measured through Phase Locked Loop (PLL) and transformed into synchronous dq frame from abc stationary frame. Representing system active power, i_{dg}^{*} reference current is obtained from PI controller for dc voltage control. With modulation index m_a, DC reference voltage can be set as given in equation 7 so as to achieve around 20% voltage adjustment margin during grid disturbances.

$$v_{dc}^{*} = \frac{\sqrt{6}v_{ai}}{m_a} \tag{7}$$

Zero reactive power reference, Q_{GSC}^{*} is applied for unity power factor operation. Without decoupled controller design, grid side converter control leads to a cross-coupled state equation for current i_{dg} in dq synchronous frame with speed ω_g as shown below:

$$\frac{di_{dg}}{dt} = (v_{dg} - v_{di} - \omega_g L_g i_{qg}) / L_g \tag{8}$$

$$\frac{di_{qg}}{dt} = (v_{qg} - v_{qi} - \omega_g L_g i_{dg}) / L_g \tag{9}$$

With PI based decoupled controller, control of d-axis and q-axis grid current becomes independent of each other as shown in equation 10 and 11, leading to better control operation.

$$\frac{di_{dg}}{dt} = (k_1 + \frac{k_2}{s})(i_{dg}^{*} - i_{dg}) / L_g \tag{10}$$

$$\frac{di_{qg}}{dt} = (k_1 + \frac{k_2}{s})(i_{qg}^{*} - i_{qg}) / L_g \tag{11}$$

More details can be obtained from [26].

V. Test System Description

A typical network connection of a wind farm with electrical grid is shown in Fig. 9 which is used for simulation tests in this study. Six DFIG based turbines, each rated 1.5 MW are used in 9 MW wind farm which is connected to 25KV distribution network. Wind farm exports power to 120 KV electrical grid through 25 kV feeder which is 30 km long. A constant wind speed at 11 m/s is applied while power electronics based IGBTs are used for converters. The wound rotor induction machine with maximum operating slip of ±20% produce rated converter voltage. The dc-link capacitors with nominal dc voltage rating of 1100 V are used for their additional surge capacity. Impact of pulsewidth modulation (PWM) switching is minimized by incorporating a three-phasechoke. Voltage disturbances are simulated at bus 120 so that near to zero voltage is experienced at bus 120 until the line is cleared of disturbances.

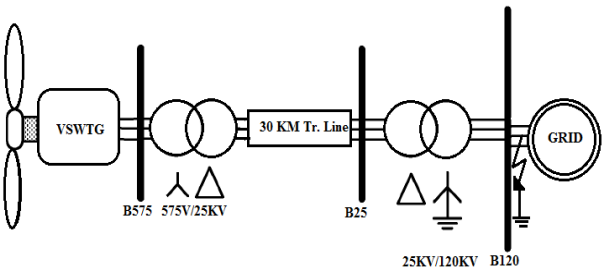

Figure 9. Test network.

VI. Simulations & Discussion

SimPower toolbox of Matlab Simulink [27] was used to simulate the test system. Test system was investigated at constant wind speed of 11 m/s for different voltage disturbance range. Simulation results for two of the most onerous cases is presented in this paper: a 10% voltage enduring for 150 ms& 450 msand0%voltageenduringfor150ms. Test cases were chosen to reflect grid-code requirements, as discussed previously.

Any comprehensive low voltage ride through technique must be capable of satisfying following three points.

- Reduced voltage drop at the generator.
- Divert or cancel rotor high currents below the surge capabilityofconverter.
- Produce appropriate power output during faults.

Simulation results for LVRT capability of FR-VSWTG shows improvement over conventional VSWTG in all the three aspects mentioned above.

Case A: $0V_{nom}$ Voltage Disturbance

It was observed that frequency responsive VSWTG was unable to sustain 0V disturbance for 450 ms and exhibits un-stability in all parameters. On the other hand they are able to sustain 0V disturbance for 150 ms without any instability.

Case B: $0.1V_{nom}$ Voltage Disturbance

Fig. 10 shows the voltage and current measured at different point of test system when voltage disturbance of $0.1V_{nom}$ is induced at bus 120 for 150ms starting at 2 seconds. As soon as voltage at point of common coupling drops to $0.1V_{nom}$, active power starts decreasing and it is at minimum level but above zero and sustain this voltage disturbance thereby avoiding shutdown. Slight variation (4-8% of nominal dc voltage) of dc link voltage is observed at the start of disturbance and after clearing of disturbance. Fig. 11 shows rotor current where we can notice high current up-to 2 p.u. for very small duration around 5 ms during and after voltage disturbance while it is around 0.9 p.u.(reference rotor voltage is 0.9p.u) during the rest of time of voltage disturbance.

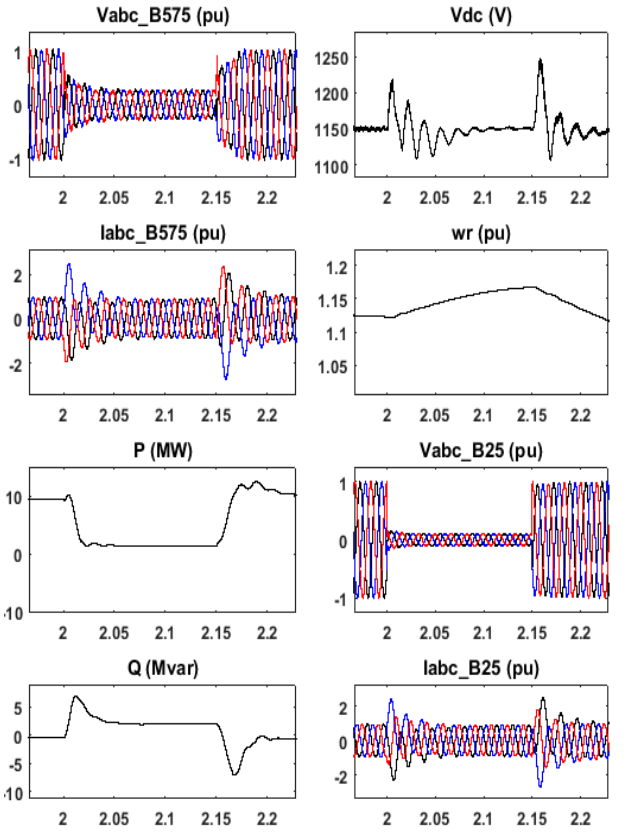

Figure 10. Simulation results for 0.1 V_{nom} for 150.

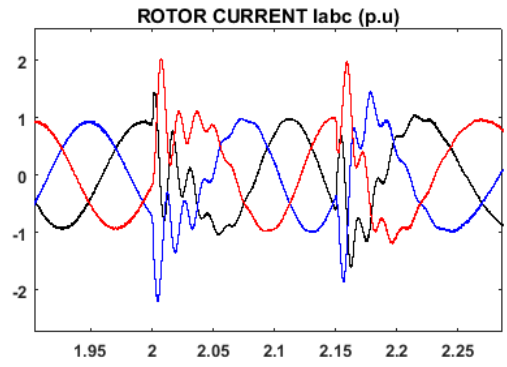

Figure 11. Rotor current during voltage disturbance.

When 0.1 V_{nom} appears at PCC at bus 120, around 0.3 p.u. voltage drop is observed at generator terminal. Fig. 12 presents the simulation results for 0.1 V_{nom} voltage drop for 450 ms. Even though rotor currents are sustained within 0.9 p.u during the vol. disturbance duration, active power recovery time is more than the previous case of 150 msec. Rotor currents increases to 1.8 p.u for 17ms after removal of voltage disturbance. Even though total currents are under 2 p.u. of maximum converter limit, additional protection device would be beneficial for this duration of disturbance.

Swift active and reactive power restoration following fault initiation and clearance is expected from any proposed FRT scheme in order to improve the fault response of other locally connected equipment, ultimately contributing to system frequency stability. Minimum active power achieved during 0 voltage drop for 150 ms is 0.3-0.4 p.u. while it around 1.3-1.4 p.u for 0.1 V drop for same duration. Active power changes from 1.5 p.u. to 0.5p.u during voltage disturbance of 0.1 V for 450 msec. Respective test results are given in Table I.

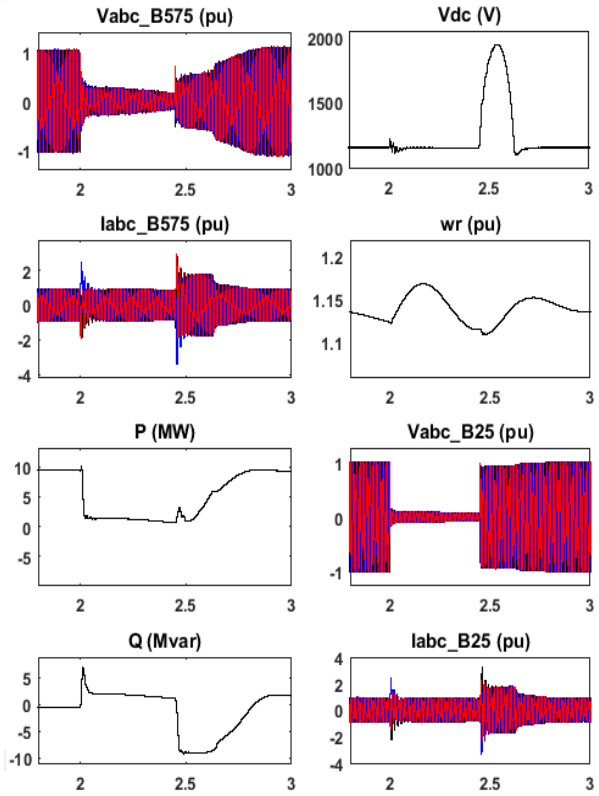

Figure 12. Simulation results for 0.1 v for 450 ms.

TABLE I. TEST RESPONSE

Voltage drop, p.u	Disturbance Duration, ms	Time to ramp up active power, s	Max. Dc link voltage, V
0.1	150	0.02	1240
0.1	450	0.35	1950
0	150	0.02	1270
0	450	Unstable	unstable

Fig. 13 shows the DFIG response during 0.1 V_{nom} voltage disturbance when it is not working in frequency controlled mode and rated 1 p.u. power is applied to pitch compensator. Differences were observed in rotor current, power ramp rate, reactive power change and rotor speed change during the voltage disturbance. Current at generator terminal is initially more than 2 p.u. and 1 p.u. during voltage disturbance while it is 0.9 p.u. with frequency responsive operation. Under similar test conditions, lower active power is achieved both before and after the disturbance (varying from 8-6.5 p.u.) in comparison to frequency responsive VSWTG (delivering 9.5 p.u. before and after disturbance). Reactive power also takes more time to settle to zero. It is also observed that rotor speed goes into super synchronous speed mode i.e.; above rated 1.2 p.u. during disturbance while it moves into sub synchronous speed mode when operating in frequency responsive mode. DC link voltage remains

the same in both case. If reference power is set to zero during voltage disturbance, normal DFIG operation fails to ride through and imbalance rotor current and high variation in dc link voltage is observed.

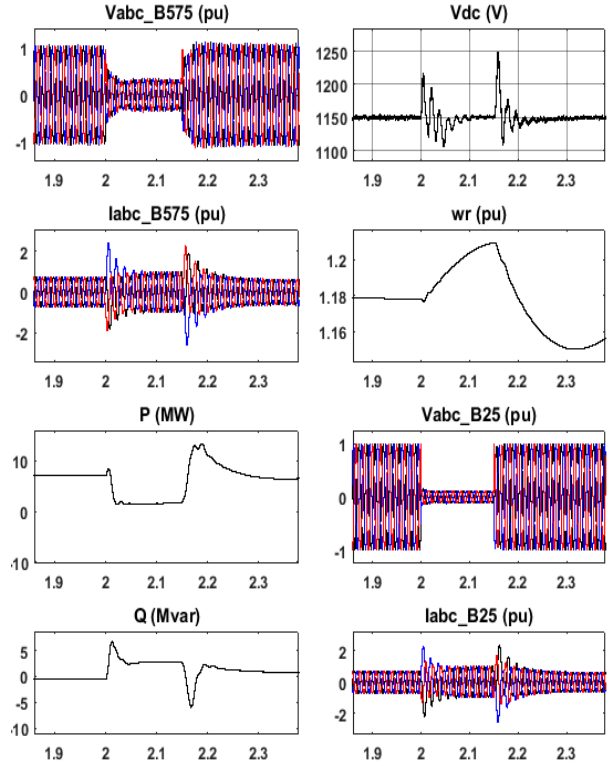

Figure 13. Simulation results for 0.1 v for 150 ms for normal DFIG Operation.

VII. Conclusion

This paper has briefly analyzed the LVRT capability of DFIG based wind plant which is operating in frequency responsive mode. Even though low priority is given to active power control in conventional DFIG operation. Simulation results show improved LVRT response when it is under frequency responsive mode with reference power varying under grid frequency and TSO limitations. Frequency responsive VSWTG is able to sustain 0 voltage drop for 150 ms which is most stringent FRT requirement among all grid codes. Under similar test conditions, frequency responsive VSWTG show improved active power output during and after fault and increased ramp up rate for active power and ramp down rate for reactive power in comparison to normal operation of DFIG. Incorporation of extra protection equipment will give robust LVRT response as well frequency responsive control. A more detail analysis must be conducted for concluding and finalizing change in active current priority threshold in frequency responsive VSWTGs.

References

[1] Z. Peng and H. Yikang, "Control strategy of an active crowbar for DFIG based wind turbine under grid voltage dips," in *Proc. International Conference on Electrical Machines and Systems*, 2007, pp. 259-264.

[2] L. Peng, B. Francois, and Y. Li, "Improved crowbar control strategy of DFIG based wind turbines for grid fault ride-through," in *Proc. APEC*, 2009, pp. 1932-1938.

[3] I. Erlich, H. Wrede, and C. Feltes "Dynamic behavior of DFIG-based wind turbines during grid faults," in *Proc. Power Conversion Conference*, Nagoya, 2007, pp. 1195-1200.

[4] J. Yang, J. E. Fletcher, and J. O'Reilly, "A series dynamic resistor based converter protection scheme for doubly-fed induction generator during various fault conditions," presented at IEEE PES GM 2009, Calgary, Canada, July 2009.

[5] J. Lopez, P. Sanchis, X. Roboam, and L. Marroyo, "Dynamic behavior of the doubly-fed induction generator during three-phase voltage dips," *IEEE Trans. Energy Conv.*, vol. 22, no. 3, pp. 709-717, Sep. 2007.

[6] A. H. Kasem, E. F. El-Saadany, and H. H. El-Tamaly, "An improved fault-ride through strategy for doubly fed induction generator based wind turbines," *IET RPG*, vol. 2, no. 4, pp. 201-214, 2008.

[7] H. N. D. Le and S. Islam, "Substantial control strategies of DFIG wind power system during grid transient faults," presented at IEEE/PES T&D, Chicago, USA, 2008.

[8] I. Erlich, H. Wrede, and C. Feltes, "Dynamic behaviour of DFIG-based wind turbines during grid faults," presented at the IEEE Power Convers. Conf., Nagoya, Japan, April 2007.

[9] A. Hansen and G. Michalke, "Fault ride-through capability of DFIG wind turbines," *Renewable Energy*, vol. 32, pp. 1594-1610, 2007.

[10] G. Pannell, D. Atkinson and B. Zahawi, "Minimum-threshold crowbar for a fault-ride-through grid-code-compliant DFIG wind turbine," *IEEE Trans. Energy Convers.*, vol. 25, no. 3, pp. 750-759, Sep. 2010.

[11] K. Okedu, "Stability enhancement of DFIG-based variable speed wind turbine with crowbar by FACTS device as per grid requirement," *International Journal of Renewable Energy Research*, vol. 2, pp. 431-439, 2012.

[12] G. Lalor, A. Mullane, and M. O'Malley, "Frequency control and wind turbine technologies," *IEEE Trans. Power Syst.*, vol. 20, no. 4, pp. 1905-1913, Nov. 2005.

[13] G. Ramtharan, J. B. Ekanayake, and N. Jenkins, "Frequency support from doubly fed induction generator wind turbines," *IET RPG*, vol. 1, no. 1, pp. 3-9, Mar. 2007.

[14] L. Holdsworth, J. B. Ekanayake, and N. Jenkins, "Power system frequency response from fixed speed and doubly fed induction generator-based wind turbines," *Wind Energy*, vol. 7, no. 1, pp. 21-35, 2004.

[15] J. Morren, J. Pierik, and S. W. H. de Haan, "Inertial response of variable speed wind turbines," *Electric Power Systems Research*, vol. 76, no. 11, pp. 980-987, Jul. 2006.

[16] M. Kayikci and J. V. Milanovic, "Dynamic contribution of DFIG-based wind plants to system frequency disturbances," *IEEE Trans. Power Syst.*, vol. 24, no. 2, pp. 859-867, May 2009.

[17] R. G. de Almeida and J. A. P. Lopes, "Participation of doubly fed induction wind generators in system frequency regulation," *IEEE Trans. Power Syst.*, vol. 22, no. 3, pp. 944-950, Aug. 2007.

[18] N. R. Ullah, T. Thiringer, and D. Karlsson, "Temporary primary frequency control support by variable speed wind turbines—Potential and applications," *IEEE Trans. Power Syst.*, vol. 23, no. 2, pp. 601-612, May 2008.

[19] F. Iov, A. D. Hansen, P. Sørensen, and N. A. Cutululis, "Mapping of grid faults and grid codes," Tech. Rep. Risø-R-1617(EN), Risø Nat. Lab., Tech. Univ. Denmark, Roskilde, Denmark, Jul. 2007.

[20] Australian Energy Market Commission (AEMC). 2009. National Electricity Rules Version 63. [Online]. Available: http://aemc.gov.au/Energy-Rules/Nationalelectricty-Version-63

[21] The Grid Code, Issue 4, Revision 10, National Grid Electricity Transmission plc, UK, January 2012.

[22] K. Clark, N. W. Miller, and J. J. Sanchez-Gasca, *Modeling of GE Wind Turbine-Generators for Grid Studies*, Version 4.5, General Electric International, Inc., April 2010.

[23] V. C. Ganti, B. Singh, S. K. Aggarwal, and T. C. Kandpal, "DFIG-based wind power conversion with grid power leveling for reduced gusts," *IEEE Transactions on Sustainable Energy*, vol. 3, no. 1, pp. 12-20, 2012.

[24] S. Chondrogiannis and M. Barnes, "Stability of doubly-fed induction generator under stator voltage orientated vector control," *IET Gen. Transm. Distrib.*, vol. 2, no. 3, pp. 170-180, 2008.

[25] L. Xu and W. Cheng, "Torque and reactive power control of a doubly fed induction machine by position sensorless scheme," *IEEE Trans. Ind. Appl.*, vol. 31, no. 3, pp. 636-642, May/Jun. 1995.
[26] B. Wu, Y. Q. Lang, N. Zargari, and S. Kouro, *Power Conversion and Control of Wind Energy Systems*, John Wiley & Sons, 26 Sep. 2011.
[27] The Math Works Inc. (2006). MATLAB, Ver. 7.2. [Online]. Available: http://www.mathworks.com.

Asma Aziz is currently pursuing the Ph.D. degree in electrical engineering at the School of Engineering, Faculty of Science, Engineering and Built Environment, Geelong, Australia. Her research interests include wind energy systems, micro grid systems, and power system control & management.

Aman MTO received his Ph.D. degree in electrical engineering from Victoria University, Melbourne, Australia. He is the Deputy Head of School and the Head of Electrical and Electronics Engineering with the School of Engineering, Deakin University, Melbourne, Australia.

Alex Stojcevski is Head of the Centre of Technology, RMIT Vietnam. His research interests are in sustainable energy systems including micro grid technologies, energy efficiency and electric vehicles, engineering education including project and problem based learning, educational leadership, and distance education.

